

---

# Robust Diffusion Models for Adversarial Purification

---

Guang Lin<sup>1,2</sup>, Zerui Tao<sup>1,2</sup>, Jianhai Zhang<sup>3</sup>, Toshihisa Tanaka<sup>1,2</sup>, and Qibin Zhao<sup>2,1,\*</sup>

<sup>1</sup>Tokyo University of Agriculture and Technology

<sup>2</sup>RIKEN Center for Advanced Intelligence Project (RIKEN AIP)

<sup>3</sup>Hangzhou Dianzi University

## Abstract

Diffusion models (DMs) based adversarial purification (AP) has shown to be the most powerful alternative to adversarial training (AT). However, these methods neglect the fact that pre-trained diffusion models themselves are not robust to adversarial attacks as well. Additionally, the diffusion process can easily destroy semantic information and generate a high quality image but totally different from the original input image after the reverse process, leading to degraded standard accuracy. To overcome these issues, a natural idea is to harness adversarial training strategy to retrain or fine-tune the pre-trained diffusion model, which is computationally prohibitive. We propose a novel robust reverse process with adversarial guidance, which is independent of given pre-trained DMs and avoids retraining or fine-tuning the DMs. This robust guidance can not only ensure to generate purified examples retaining more semantic content but also mitigate the accuracy-robustness trade-off of DMs for the first time, which also provides DM-based AP an efficient adaptive ability to new attacks. Extensive experiments are conducted on CIFAR-10, CIFAR-100 and ImageNet to demonstrate that our method achieves the state-of-the-art results and exhibits generalization against different attacks.

## 1 Introduction

Deep neural networks (DNNs) have been shown to be vulnerable to adversarial examples (Szegedy et al., 2014), leading to disastrous implications. Since then, numerous methods have been proposed to defend against adversarial examples. Notably, adversarial training (AT, Goodfellow et al., 2015; Madry et al., 2018a) enhances classifiers by training with adversarial examples, achieving the state-of-the-art robustness against known attacks. However, when faced with unseen attacks, AT is almost incapable of defense (Laidlaw et al., 2021; Dolatabadi et al., 2022). Another class of defense methods, adversarial purification (AP, Yoon et al., 2021), relies on pre-trained generative models to eliminate perturbations from potentially attacked images before classification. AP operates as a pre-processing step against unseen attacks without the need to retrain the classifier. Recently, by leveraging the great generative capability of diffusion models (DMs, Ho et al., 2020; Song et al., 2020), Nie et al. (2022) achieved remarkable performance using AP and was shown to be a promising alternative to AT.

However, recent studies (Lee and Kim, 2023; Kang et al., 2023; Chen et al., 2024) find that DM-based AP is not as robust as shown in previous literature (Nie et al., 2022; Wang et al., 2022). Indeed, it might be easily fooled by attacks such as PGD+EOT. Moreover, by adding Gaussian noise, the perturbation is gradually destroyed, thereby enhancing the robust accuracy, but increasing Gaussian noise can also lead to a loss of semantic information, resulting in degraded accuracy. As a remedy, Wang et al. (2022); Zhang et al. (2024) propose the reverse processes with guidance to preserve semantic information. However, their guidance only considers suppressing example information loss, which lacks robustness against adversarial example information and has a risk of preserving or even enhancing adversarial perturbations. We argue that this is caused by the non-robustness of guidance,

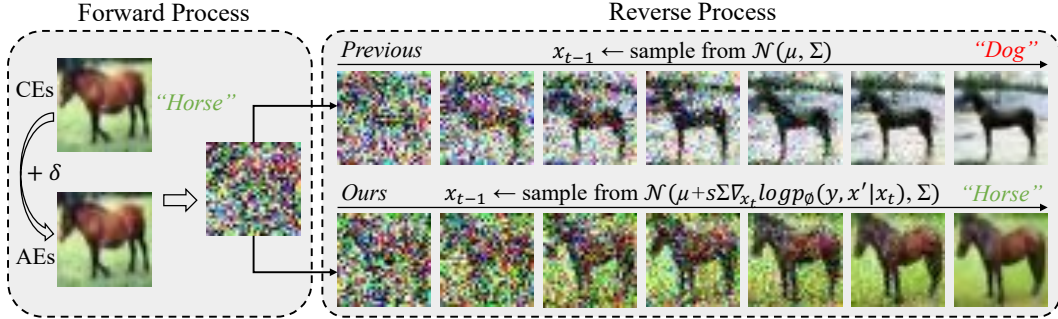


Figure 1: The scheme of diffusion-based AP. The examples are firstly diffused with Gaussian noises by the forward process and then followed by the reverse process to remove the noise step by step.

which is a crucial issue that needs to be solved. Therefore, our goal is to develop a diffusion model that can preserve semantic information while being robust to adversarial information.

To obtain a robust generator-based purifier, one possible solution is fine-tuning the generative model using adversarial examples and classification loss by freezing the classifier, which can thus preserve semantic information even under adversarial attacks. In particular, Lin et al. (2024) propose a defense pipeline called adversarial training on purification (AToP), which employs the adversarial loss to fine-tune the whole purifier and achieves great success in fine-tuning a robust AE-based purifier (Wu et al., 2023) and GAN-based purifier (Ughini et al., 2022). However, Lin et al. (2024) claim that AToP cannot work on DMs due to the high computational cost of generating adversarial examples for DMs. Therefore, the robustness of the DM-based purifier model still remains challenging.

In this paper, we propose a novel adversarial guided diffusion model (AGDM) that employs a robust reverse process with adversarial guidance of given pre-trained DMs, as illustrated in Figure 1. Notably, this robust guidance is independent of DMs and avoids retraining or fine-tuning the whole DMs. To achieve this, instead of training DMs, we train a robust guidance with a new adversarial loss and then apply this robust guidance to the reverse process of DMs during purification. Since our method does not need to compute the entire reverse process during training of robust guidance, it avoids the computational issue of AToP. Given the robust guidance, the modified reverse process of DMs can not only generate better purified examples retaining more semantic content but also mitigate the accuracy-robustness trade-off. To the best of our knowledge, this is the first approach to consider accuracy-robustness trade-off in pre-trained generator-based AP, which might be a significant contribution to advance the development of this field.

To demonstrate the effectiveness of our method, we empirically evaluate the performance by comparing with the latest AT and AP methods across various attacks, including AutoAttack (Croce and Hein, 2020), StAdv (Xiao et al., 2018), PGD (Madry et al., 2018b) and EOT (Athalye et al., 2018), on CIFAR-10, CIFAR-100 and ImageNet datasets under multiple classifier models. The experimental results demonstrate that our method achieves the state-of-the-art performance on both accuracy and robustness among AP baselines. Moreover, our method exhibits better robust generalization against unseen attacks. More importantly, our results on the robust evaluation of diffusion-based purification (Lee and Kim, 2023) manifest the necessity of robust guidance in diffusion models for adversarial purification. Our contributions are summarized as follows.

- To enhance the robustness of diffusion models, we propose a robust reverse process to preserve semantic information and generate robust purified examples.
- An adversarial loss is proposed to train robust guidance, thus subtly bypassing the high computational demand when applying AT to DMs. It also provides a practical solution to mitigate the accuracy-robustness trade-off in DM-based AP.
- We conduct extensive experiments to empirically demonstrate that the proposed method significantly improves both the accuracy and robustness of diffusion-based purifier models, especially under the new robust evaluation scheme (Lee and Kim, 2023).

## 2 Preliminary

This section briefly review the adversarial training, adversarial purification, and diffusion models.

## 2.1 Adversarial Training and Adversarial Purification

Given a classifier  $c_\gamma$  with input  $x$  and output  $y$ , the adversarial attacks aim to find the adversarial examples  $x'$  that can fool the classifier model  $c_\gamma$ . The adversarial examples can be obtained by

$$x' = x + \delta, \quad \delta = \arg \max_{\delta \leq \varepsilon} \mathcal{L}(c_\gamma(x + \delta), y),$$

where  $\delta$  represents a small perturbation and  $\varepsilon$  represents the maximum scale. To defend against adversarial attacks, the most popular technique is adversarial training (AT, Goodfellow et al., 2015; Madry et al., 2018a), which requires the classifier  $c_\gamma$  to be retrained with adversarial examples by

$$\min_{\gamma} \mathbb{E}_{p_{\text{data}}(x, y)} [\max_{\delta \leq \varepsilon} \mathcal{L}(c_\gamma(x + \delta), y)].$$

Another technique is adversarial purification (AP, Yang et al., 2019; Shi et al., 2021), which can purify the adversarial examples before feeding them into the classifier model, i.e.,

$$c_\gamma(g_\theta(x + \delta)) = c_\gamma(x),$$

where the purifier model  $g_\theta$  in general does not require  $g_\theta(x + \delta) = x$ . As a plug-and-play module, the pre-trained generator-based purifier model can be integrated with any classifiers.

## 2.2 Diffusion Models

Diffusion models (Ho et al., 2020; Song et al., 2020) are a class of generative models that can generate high-quality images, which consist of two processes: a forward process transforms an image entirely into noise by gradually adding Gaussian noise, and a reverse process transforms noise into the generated image by gradually denoising.

In the denoising diffusion probabilistic model (DDPM, Ho et al., 2020), given a real image  $x_0 \sim q(x)$ , the forward process involves  $T$  steps, resulting in  $x_1, x_2, \dots, x_T$ . Since each step  $t$  is only related to the previous step  $t - 1$ , it can also be viewed as a Markov process,

$$q(x_t | x_{t-1}) = \mathcal{N}(x_t; \sqrt{1 - \beta_t}x_{t-1}, \beta_t \mathbf{I}),$$

$$q(x_{1:T} | x_0) = \prod_{t=1}^T q(x_t | x_{t-1}),$$

where  $\beta_t$ , as a hyperparameter, is typically set to linearly interpolate from 0.0001 to 0.02 (Nichol et al., 2022). With  $\alpha_t := 1 - \beta_t$  and  $\bar{\alpha}_t := \prod_{s=1}^t \alpha_s$ , any step  $t$  can be rewritten as one direct sample from

$$q(x_t | x_0) = \mathcal{N}(x_t; \sqrt{\bar{\alpha}_t}x_0, (1 - \bar{\alpha}_t)\mathbf{I}). \quad (1)$$

The reverse process aims to restore the original image  $x_0$  from the Gaussian noise  $x_T \sim \mathcal{N}(0, \mathbf{I})$  by sampling from  $p_\theta(x_{t-1} | x_t)$ , given by

$$p_\theta(x_{t-1} | x_t) = \mathcal{N}(x_{t-1}; \mu_\theta(x_t, t), \sigma_t^2 \mathbf{I}),$$

$$p_\theta(x_{0:T}) = p(x_T) \prod_{t=T}^1 p_\theta(x_{t-1} | x_t),$$

where  $\sigma_t$  denotes a time dependent constant and  $\mu_\theta(x_t, t) = \frac{1}{\sqrt{\bar{\alpha}_t}}x_t - \frac{1 - \alpha_t}{\sqrt{1 - \bar{\alpha}_t}\sqrt{\alpha_t}}\epsilon_\theta$  is usually modeled by a U-Net  $\epsilon_\theta$ , which needs to be trained to predict a random noise at each time step by Ho et al. (2020),

$$L(\theta) = \mathbb{E}_{t, x_0, \epsilon} [\|\epsilon - \epsilon_\theta(\sqrt{\bar{\alpha}_t}x_0 + \sqrt{1 - \bar{\alpha}_t}\epsilon, t)\|^2],$$

where  $\epsilon \sim \mathcal{N}(0, \mathbf{I})$  denotes a Gaussian noise. Unlike the forward process, which can be directly computed by Equation (1), the reverse process requires  $T$  steps to obtain  $x_0$  from  $x_T$ . Therefore, as compared to other generative models, diffusion models are much slower in image generation.

## 3 Methods

We propose a novel adversarial guided diffusion model (AGDM) for adversarial purification, which purifies adversarial examples by a robust reverse process. We derive our method in Section 3.1. Then, we discuss how to train a robust classifier and mitigate the accuracy-robustness trade-off in Section 3.2. Finally, we introduce the whole process of our diffusion-based purification in Section 3.3.

### 3.1 Adversarial Guided Diffusion Model

Unlike the guided diffusion (Dhariwal and Nichol, 2021; Wu et al., 2022; Kim et al., 2023; Zhang et al., 2024), we are the first to introduce a robust classifier guidance to the reverse process. Similar to Dhariwal and Nichol (2021), we have

$$p_{\theta, \phi}(x_t | x_{t+1}, y, x') \propto p_{\theta}(x_t | x_{t+1})p_{\phi}(x' | x_t)p_{\phi}(y | x_t), \quad (2)$$

where  $x'$  is the adversarial example. To obtain this factorization of probabilities, we assume the label  $y$  and adversarial example  $x'$  are conditionally independent given  $x_t$ . The conditional distribution  $p_{\theta}(x_t | x_{t+1})$  is characterized by the pre-trained diffusion model, while  $p_{\phi}(x' | x_t)p_{\phi}(y | x_t)$  can be modeled by a robust classifier. In specific,  $p_{\phi}(y | x_t)$  is the prediction of labels. Moreover, to describe relations between adversarial and diffused clean images, we adopt a heuristic probability,

$$p_{\phi}(x' | x_t) \propto \exp(-\mathcal{D}(f_{\phi}(x'), f_{\phi}(x_t))),$$

where  $\mathcal{D}(\cdot, \cdot)$  is distance measurement and  $f_{\phi}$  is the classifier function that outputs the logit of labels.

For the first term in Equation (2), we have

$$\log p_{\theta}(x_t | x_{t+1}) = -\frac{1}{2}(x_t - \mu)^{\top} \Sigma^{-1} (x_t - \mu) + C_1, \quad (3)$$

where  $\mu$  and  $\Sigma$  are obtained by the pre-trained diffusion model and  $C_1$  is a constant w.r.t.  $x_t$ . We omit the inputs of the function for clarity, consistent with notations with Dhariwal and Nichol (2021). The second term in Equation (2) can be approximated as

$$\begin{aligned} \log p_{\phi}(x' | x_t) &\approx \log p_{\phi}(x' | x_t) |_{x_t=\mu} + (x_t - \mu)^{\top} \nabla_{x_t} \log p_{\phi}(x' | x_t) |_{x_t=\mu} \\ &= (x_t - \mu)^{\top} \nabla_{x_t} \mathcal{D}(f_{\phi}(x'), f_{\phi}(x_t)) + C_2, \end{aligned} \quad (4)$$

where  $C_2$  is a constant w.r.t.  $x_t$ . Finally, for the last term in Equation (2), we have

$$\begin{aligned} \log p_{\phi}(y | x_t) &\approx \log p_{\phi}(y | x_t) |_{x_t=\mu} + (x_t - \mu)^{\top} \nabla_{x_t} \log p_{\phi}(y | x_t) |_{x_t=\mu} \\ &= (x_t - \mu)^{\top} g + C_3, \end{aligned} \quad (5)$$

where  $g = \nabla_{x_t} \log p_{\phi}(y | x_t)$  and  $C_3$  is a constant w.r.t.  $x_t$ . By plugging Equations (3) to (5) into Equation (2), we obtain the adjusted score function with robust guidance,

$$\log p_{\theta, \phi}(x_t | x_{t+1}, y, x') = \log p(z) + C_4,$$

where  $C_4$  is a constant and  $z$  follows

$$z \sim \mathcal{N}(z; \mu + \Sigma g - \Sigma \nabla_{x_t} \mathcal{D}(f_{\phi}(x'), f_{\phi}(x_t)), \Sigma).$$

The full derivation is shown in Appendix A.1. The above derivation of guided sampling is valid for DDPM. However, the robust reverse process can be extended to continuous-time diffusion models. Specifically, the denoising model  $\epsilon_{\theta}$  can be used to derive a score function (Song et al., 2020; Dhariwal and Nichol, 2021). Consider a diffusion process with drift coefficient  $f(x, t)$  and diffusion coefficient  $G(t)$ , the robust reverse process becomes (details in Appendix A.2)

$$dx_t = [f(x, t) - G^2(t)(s_{\theta} + a_{\phi} + b_{\phi})(x, t)] dt + G(t) d\bar{w},$$

where  $s_{\theta}(x, t)$  is the pre-trained score network,  $a_{\phi}(x, t) = \nabla_{x_t} \log p_{\phi}(y | x_t)$  and  $b_{\phi}(x, t) = \nabla_{x_t} \log p_{\phi}(x' | x_t)$ . The proposed reverse process with robust guidance is presented in Algorithm 1. Note that a key challenge is to obtain the robust guidance for diffusion models. As we explained before, generating adversarial examples for the diffusion model as in Lin et al. (2024) is infeasible. In the next subsection, we address this issue by a modification of the adversarial loss in Lin et al. (2024).

### 3.2 Robust Guidance Training

According to the above contents and adversarial training (Zhang et al., 2019), we train another robust classifier with classification loss on clean examples  $x$  and discrepancy loss on adversarial examples  $x'$  and clean examples  $x$ ,

$$\min_{\phi} \mathbb{E}_{p_{\text{data}}(x, y)} \left[ \underbrace{\mathcal{L}(f_{\phi}(x), y)}_{\text{for accuracy}} + \lambda \underbrace{\max_{\delta \leq \epsilon} \mathcal{D}(f_{\phi}(x), f_{\phi}(x'))}_{\text{for robustness}} \right], \quad (6)$$

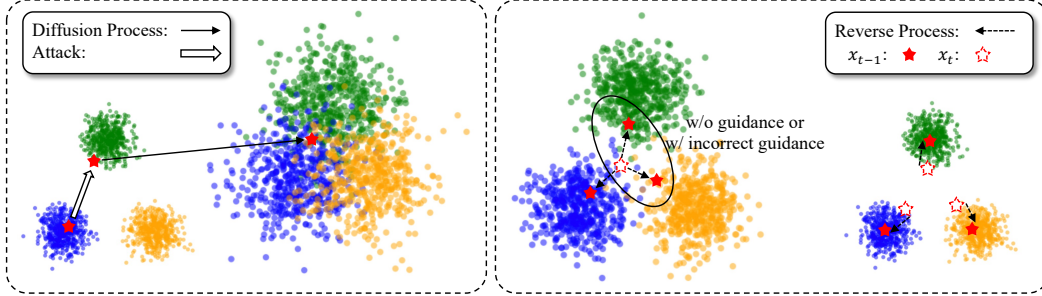


Figure 2: Overview of the diffusion process and reverse process. The movement of the red star represents the entire purification process. Different colored dots represent the data distributions of various categories. In the presence of attacks, without guidance or with incorrect guidance, the red star may move to the wrong category in the reverse process, thereby reducing robust accuracy.

where  $x' = x + \delta$ , and  $\lambda$  is a weighting scale to balance the accuracy-robustness trade-off.

Unlike the previous work (Lin et al., 2024), they calculate the classification loss with adversarial examples  $\mathcal{L}(f_\phi(x'), y)$  for fine-tuning to improve robust accuracy. Instead, we introduce discrepancy loss  $\mathcal{D}(f_\phi(x), f_\phi(x'))$  to improve robustness while using only clean examples to calculate the classification loss  $\mathcal{L}(f_\phi(x), y)$  to improve standard accuracy, details in Appendix B. To our best knowledge, this is the first to discuss the accuracy-robustness trade-off challenge in pre-trained generator-based purification.

### 3.3 Robust Reverse Process

The vanilla reverse process is vulnerable to adversarial attacks (Lee and Kim, 2023). During attacks, the vanilla classifier (Zhang et al., 2024) may provide incorrect gradients, leading to incorrect guidance. Likewise, the reverse process without guidance can also lead to the sampling of noisy images towards incorrect labels, as shown in Figure 2. Considering this issue, we introduce additional adversarial information to sampling image from the robust reverse process.

Given an adversarial example  $x'$ , we first diffuse  $x'$  with  $t^*$  steps by

$$x_{t^*} = \sqrt{\bar{\alpha}_{t^*}} x' + \sqrt{1 - \bar{\alpha}_{t^*}} \epsilon, \quad \epsilon \sim \mathcal{N}(0, \mathbf{I}). \quad (7)$$

Then, in the robust reverse process, we can obtain the purified example  $x_0$  by sampling  $x_{t-1}$  from  $\mathcal{N}(\mu + s \Sigma \nabla_{x_t} \log p_\phi(y, x' | x_t), \Sigma)$  with  $t^*$  steps. Note that we add scale  $s$  to adjust the guidance, which can be regarded as a temperature (Kingma and Dhariwal, 2018) in the distribution, i.e.,  $p_\phi(x' | x_t)^s p_\phi(y | x_t)^s$ .

## 4 Related Work

**Adversarial training (AT)** is initially proposed by Goodfellow et al. (2015) to defend against adversarial attacks. While adversarial training has been demonstrated as an effective defend against attacks, it remains susceptible to unseen attacks (Stutz et al., 2020; Poursaeed et al., 2021; Laidlaw et al., 2021; Tack et al., 2022). Additionally, retraining the classifier model with only adversarial examples could severely impair the standard accuracy of the model (Kurakin et al., 2016; Madry et al., 2018b). To address this issue, Zhang et al. (2019); Pang et al. (2022) propose the loss functions that can effectively mitigate the trade-off between robustness and clean accuracy.

**Adversarial purification (AP)** purifies adversarial examples before classification, which has emerged as a promising defense method (Shi et al., 2021; Srinivasan et al., 2021). Compared with the AT method, AP utilizes a pre-trained generator that can defend against unseen attacks without retraining the classifier model (Song et al., 2018; Samangouei et al., 2018; Schott et al., 2019). For instance, Ughini et al. (2022) utilize a GAN-based generator and Nie et al. (2022) utilize a diffusion-based generator for adversarial purification. However, pre-trained generator-based AP methods cannot be adapted to known or new attacks, as the generator is trained without adversarial examples (Lee and Kim, 2023). To address this issue, Lin et al. (2024) propose adversarial training on purification (AToP), which fine-tunes the generator, enabling it to effectively defend against new attacks. However,

the computational cost of AToP is highly related to the complexity of the generator model, rendering it impractical for application to diffusion models.

**Diffusion model (DM)** is a powerful generative model, achieving high-quality image generation (Ho et al., 2020; Song et al., 2020). Motivated by the great success of DMs, Yoon et al. (2021); Nie et al. (2022); Xiao et al. (2023); Carlini et al. (2023) utilize a pre-trained DM for adversarial purification and provided theoretical analysis, which acts as a solid foundation for diffusion-based purification. To better preserve semantic information, Wu et al. (2022); Wang et al. (2022) propose guided diffusion model for adversarial purification. Following a similar intention, Zhang et al. (2024) proposes a classifier-guided diffusion model to ensure the restoration of images with the target label.

However, all of the diffusion-based purification models do not consider the robustness of DMs, as shown in Lee and Kim (2023) and our experiments. In the presence of attacks, the model can produce incorrect guidance, leading to a decrease in accuracy. Unlike previous works, we improve the inherent robustness of DMs by proposing a novel robust reverse process with adversarial guidance.

## 5 Experiments

In this section, we conduct extensive experiments on CIFAR-10, CIFAR-100 and ImageNet across various classifier models on attack benchmarks. Compared with the state-of-the-art methods, our method achieves optimal performance and exhibits generalization ability against unseen attacks. Furthermore, we undertake a more comprehensive evaluation scheme (Lee and Kim, 2023). Our method achieves the optimal average robust accuracy against PGD+EOT and AutoAttack.

### 5.1 Experimental Setup

**Datasets and classifiers:** We conduct extensive experiments on CIFAR-10, CIFAR-100 (Krizhevsky et al., 2009) and ImageNet (Deng et al., 2009) to empirically validate the effectiveness of the proposed methods against adversarial attacks. For the classifier models, we utilize the pre-trained ResNet (He et al., 2016) and WideResNet (Zagoruyko and Komodakis, 2016).

**Adversarial attacks:** We evaluate our method against AutoAttack (Croce and Hein, 2020) as one benchmark, which is a powerful attack that combines both white-box and black-box attacks. To consider unseen attacks without  $l_p$ -norm, we utilize spatially transformed adversarial examples (StAdv, Xiao et al., 2018) for evaluation. Additionally, following the guidance of Lee and Kim (2023), we utilize projected gradient descent (PGD, Madry et al., 2018b) with expectation over time (EOT, Athalye et al., 2018) for a more comprehensive evaluation of the diffusion-based purification.

**Evaluation metrics:** We evaluate the performance of defense methods using two metrics: standard accuracy and robust accuracy, obtained by testing on clean examples and adversarial examples, respectively. Due to the high computational cost of testing models with multiple attacks, following guidance by Nie et al. (2022), we randomly select 512 images from the test set for robust evaluation.

**Training details:** According to Zhang et al. (2019); Dhariwal and Nichol (2021) and experiments, we set the scale  $s = 1.0$ , and the weighting scale  $\lambda = 6.0$ . Unless otherwise specified, all experiments presented in the paper are conducted under these hyperparameters and done using the NVIDIA RTX A5000 with 24GB GPU memory and CUDA v11.7 in PyTorch v1.13.1 (Paszke et al., 2019).

### 5.2 Comparison with the State-of-the-art Methods

We evaluate our method on defending against AutoAttack  $l_\infty$  and  $l_2$  threat models (Croce and Hein, 2020), and compare with the state-of-the-art methods as listed in RobustBench (Croce et al., 2021). In all experiments presented in this section, we set the diffusion timestep  $t^* = 70$ .

**Result analysis on CIFAR-10:** Table 1 shows the performance of the defense methods against AutoAttack  $l_\infty$  ( $\epsilon = 8/255$ ) threat model on CIFAR-10 with WideResNet-28-10. Our method outperforms all other methods without extra data (the dataset introduced by Carmon et al. (2019)) and additional synthetic data in terms of both standard accuracy and robust accuracy. Specifically, as compared to the second-best method, our method improves the robust accuracy by 5.07% and the standard accuracy by 0.78%. Table 2 shows the performance of the defense methods against AutoAttack  $l_2$  ( $\epsilon = 0.5$ ) threat model on CIFAR-10 with WideResNet-28-10. Our method outperforms

Table 1: Standard and robust accuracy against AutoAttack  $l_\infty$  threat ( $\epsilon = 8/255$ ) on CIFAR-10. ( $\dagger$ the methods use additional synthetic images.)

Defense method	Extra data	Standard Acc.	Robust Acc.
Zhang et al. (2020)	✓	85.36	59.96
Gowal et al. (2020)	✓	89.48	62.70
Bai et al. (2023)	✓ <sup>†</sup>	95.23	68.06
Gowal et al. (2021)	× <sup>†</sup>	88.74	66.11
Wang et al. (2023)	× <sup>†</sup>	93.25	70.69
Peng et al. (2023)	× <sup>†</sup>	93.27	71.07
Nie et al. (2022)	×	89.02	70.64
Wang et al. (2022)	×	84.85	71.18
Zhang et al. (2024)	×	90.04	73.05
Ours	×	90.82	<b>78.12</b>

Table 4: Robust accuracy against AutoAttack  $l_\infty$  threat ( $\epsilon = 8/255$ ) and  $l_2$  threat ( $\epsilon = 0.5$ ). (<sup>1</sup>the method without guidance, <sup>2</sup>the method with guidance, <sup>3</sup>the method with robust guidance.)

Defense method	CIFAR 10, $l_\infty$	CIFAR 10, $l_2$	CIFAR 100, $l_\infty$
Nie et al. (2022) <sup>1</sup>	71.03	78.58	42.19
Zhang et al. (2024) <sup>2</sup>	73.05	83.13	40.62
Ours <sup>3</sup>	<b>78.12</b>	<b>86.84</b>	<b>46.09</b>

Table 2: Standard and robust accuracy against AutoAttack  $l_2$  threat ( $\epsilon = 0.5$ ) on CIFAR-10.

Defense method	Extra data	Standard Acc.	Robust Acc.
Augustin et al. (2020)	✓	92.23	77.93
Gowal et al. (2020)	✓	94.74	80.53
Wang et al. (2023)	× <sup>†</sup>	95.16	83.68
Ding et al. (2019)	×	88.02	67.77
Rebuffi et al. (2021)	×	91.79	78.32
Zhang et al. (2024)	×	92.58	83.13
Lee and Kim (2023)	×	90.16	86.48
Ours	×	90.82	<b>86.84</b>

Table 3: Standard and robust accuracy against AutoAttack  $l_\infty$  ( $\epsilon = 8/255$ ) on CIFAR-100.

Defense method	Extra data	Standard Acc.	Robust Acc.
Hendrycks et al. (2019)	✓	59.23	28.42
Debenedetti et al. (2023)	✓	70.76	35.08
Cui et al. (2023)	× <sup>†</sup>	73.85	39.18
Wang et al. (2023)	× <sup>†</sup>	75.22	42.67
Pang et al. (2022)	×	63.66	31.08
Jia et al. (2022)	×	67.31	31.91
Cui et al. (2023)	×	65.93	32.52
Ours	×	69.73	<b>46.09</b>

all methods in terms of robust accuracy. Specifically, as compared to the second-best method, our method improves the robust accuracy by 0.36%. These results demonstrate that our method achieves the state-of-the-art performance in RobustBench (Croce et al., 2021).

**Result analysis on CIFAR-100:** Table 3 shows the performance of the defense methods against AutoAttack  $l_\infty$  ( $\epsilon = 8/255$ ) threat model on CIFAR-100 with WideResNet-28-10. Our method outperforms all other methods without synthetic data in terms of both standard accuracy and robust accuracy. Specifically, as compared to the second-best method, our method improves the robust accuracy by 3.42%. The observations are basically consistent with CIFAR-10, further demonstrating the effectiveness of our method for adversarial purification.

**Result analysis on guidance:** Table 4 shows the robust accuracy of the three guidance patterns of diffusion model, i.e., the method without guidance (Nie et al., 2022), the method with guidance (Zhang et al., 2024), and the method with robust guidance (ours). Our method achieves optimal

Table 5: Standard accuracy and robust accuracy against AutoAttack  $l_\infty$  ( $\epsilon = 8/255$ ),  $l_2$  ( $\epsilon = 1$ ) and StAdv non- $l_p$  ( $\epsilon = 0.05$ ) threat models on CIFAR-10 with ResNet-50 model. We keep the same settings with Nie et al. (2022), where the diffusion timestep  $t^* = 125$ .

Defense method	Standard Acc.	AA $l_\infty$	AA $l_2$	StAdv
Standard Training	94.8	0.0	0.0	0.0
Adv. Training with $l_\infty$ (Laidlaw et al., 2021)	86.8	49.0	19.2	4.8
Adv. Training with $l_2$ (Laidlaw et al., 2021)	85.0	39.5	47.8	7.8
Adv. Training with StAdv (Laidlaw et al., 2021)	86.2	0.1	0.2	53.9
Adv. Training with all (Laidlaw et al., 2021)	84.0	25.7	30.5	40.0
PAT-self (Laidlaw et al., 2021)	82.4	30.2	34.9	46.4
Adv. CRAIG (Dolatabadi et al., 2022)	83.2	40.0	33.9	49.6
DiffPure (Nie et al., 2022)	88.2	70.0	70.9	55.0
AGDM (Ours)	89.3	<b>78.1</b>	<b>79.6</b>	<b>59.4</b>

robustness under all situations. Specifically, our method improves the robust accuracy by 5.07% against AutoAttack  $l_\infty$ , and by 3.71% against AutoAttack  $l_2$  on CIFAR-10, respectively. Furthermore, it shows an improvement of 3.9% on CIFAR-100. The results demonstrate that our method can significantly improve the robustness of the pre-trained diffusion-based purifier model.

**Result analysis on unseen attacks:** As previously mentioned, unlike AT, AP can defend against unseen attacks, which is an important metric for evaluating AP. To demonstrate the generalization ability of AGDM, we conduct experiments under several different attacks with varying constraints (AutoAttack  $l_\infty$ ,  $l_2$  and StAdv non- $l_p$  threat models) on CIFAR-10 with ResNet-50. Table 5 shows that AT methods are limited in defending against unseen attacks and can only defend against known attacks (as indicated by the accuracy with an underscore) that they are trained with. In contrast, diffusion-based AP (DiffPure, Nie et al., 2022) demonstrates generalization capabilities to defend against all attacks. Our method further outperforms DiffPure in all situations. Specifically, it improves the robust accuracy by 8.1%, 8.7%, and 4.4% on AutoAttack  $l_\infty$ ,  $l_2$  and StAdv non- $l_p$ , respectively. The results demonstrate that our method exhibits better generalization ability against unseen attacks.

### 5.3 Robust Evaluation of Diffusion-based Purification

AutoAttack is regarded as one of the strongest adversarial attacks and is acknowledged as a benchmark for evaluating various defense methods, as demonstrated in Section 5.2. However, Lee and Kim (2023) find that AutoAttack may not effectively evaluate the robustness of diffusion-based AP. Following the suggestions made by Croce et al. (2022), Lee and Kim (2023) provide a new pipeline (PGD+EOT) particularly for measuring the robustness of diffusion-based purification methods against adversarial attacks. To undertake a more comprehensive evaluation, we evaluate our method defenses against  $l_\infty$  and  $l_2$  threat models following the guideline of Lee and Kim (2023) in this subsection.

Table 6: Standard and robust accuracy against PGD+EOT (left:  $l_\infty$ ,  $\epsilon = 8/255$ ; right:  $l_2$ ,  $\epsilon = 0.5$ ) on CIFAR-10. We keep the same settings with Lee and Kim (2023), the diffusion timestep  $t^* = 100$ . (<sup>1</sup>the method without guidance, <sup>2</sup>the method with guidance, <sup>3</sup>the method with robust guidance.)

Type	Defense method	Standard Acc.	Robust Acc.	Type	Defense method	Standard Acc.	Robust Acc.
WideResNet-28-10				WideResNet-28-10			
AT	Pang et al. (2022)	88.62	64.95	AT	Sehwag et al. (2021)	90.93	83.75
	Gowal et al. (2020)	88.54	65.93		Rebuffi et al. (2021)	91.79	85.05
	Gowal et al. (2021)	87.51	66.01		Augustin et al. (2020)	93.96	86.14
AP	Wang et al. (2022) <sup>2</sup>	93.50	24.06	AP	Wang et al. (2022) <sup>2</sup>	93.50	-
	Yoon et al. (2021)	85.66	33.48		Yoon et al. (2021)	85.66	73.32
	Nie et al. (2022) <sup>1</sup>	90.07	46.84		Nie et al. (2022) <sup>1</sup>	91.41	79.45
	Lee and Kim (2023)	90.16	55.82		Lee and Kim (2023)	90.16	83.59
	Ours <sup>3</sup>	90.42	<b>64.06</b>		Ours <sup>3</sup>	90.42	<b>85.55</b>
WideResNet-70-16				WideResNet-70-16			
AT	Gowal et al. (2020)	91.10	68.66	AT	Rebuffi et al. (2021)	92.41	86.24
	Gowal et al. (2021)	88.75	69.03		Gowal et al. (2020)	94.74	88.18
	Rebuffi et al. (2021)	92.22	69.97		Rebuffi et al. (2021)	95.74	89.62
AP	Yoon et al. (2021)	86.76	37.11	AP	Yoon et al. (2021)	86.76	75.66
	Nie et al. (2022)	90.43	51.13		Nie et al. (2022)	92.15	82.97
	Lee and Kim (2023)	90.53	56.88		Lee and Kim (2023)	90.53	83.75
	Ours	90.43	<b>66.41</b>		Ours	90.43	<b>85.94</b>

**Result analysis on PGD+EOT:** Table 6 shows the performance of the defense methods against PGD+EOT  $l_\infty$  ( $\epsilon = 8/255$ ) and  $l_2$  ( $\epsilon = 0.5$ ) threat models on CIFAR-10 with WideResNet-28-10 and WideResNet-70-16. Our method outperforms all AP methods in terms of robust accuracy. Specifically, as compared to the second-best method, our method improves the robust accuracy by 8.24%, 9.53% against  $l_\infty$  and by 1.96%, 2.19% against  $l_2$ , respectively. Table 7 shows the results on ImageNet and the observations are basically consistent with Table 6. These results demonstrate that our method achieves the state-of-the-art robustness in adversarial purification.



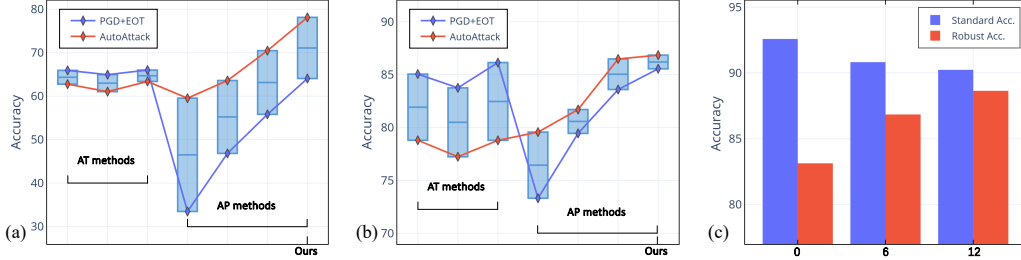


Figure 3: Comparison of robust accuracy against PGD+EOT and AutoAttack with (a)  $l_\infty$  ( $\epsilon = 8/255$ ) threat model and (b)  $l_2$  ( $\epsilon = 0.5$ ) threat model on CIFAR-10 with WideResNet-28-10. The line in the middle of the box represents the average robust accuracy of two attacks. (c) Accuracy-robustness trade-off against AutoAttack  $l_2$  ( $\epsilon = 0.5$ ) threat model on CIFAR-10 with WideResNet-28-10.

Table 7: Standard accuracy and robust accuracy against PGD+EOT  $l_\infty$  ( $\epsilon = 4/255$ ) on ImageNet with ResNet-50. The diffusion timestep  $t^* = 75$ .

Type	Defense method	Standard Acc.	Robust Acc.
AT	Wong et al. (2019)	53.83	28.04
	Engstrom et al. (2019)	62.42	33.20
	Salman et al. (2020)	63.86	39.11
AP	Nie et al. (2022)	71.48	38.71
	Lee and Kim (2023)	70.74	42.15
	Ours	68.75	<b>45.90</b>

**Result analysis on guidance:** Furthermore, Table 6 also presents the results of three guidance patterns of diffusion model, i.e., the method without guidance (Nie et al., 2022), the method with guidance (Wang et al., 2022), and the method with robust guidance (ours). Due to the presence of guidance, the reverse process can generate better images without changing their semantic content, thereby improving classification accuracy. When without attacks, the method with guidance is highly effective, which has a 3.43% increase in standard accuracy. However, they neglect the impact of attacks on guidance, leading to a 22.78% decrease in robust accuracy

when facing attacks with full gradient. In contrast, our robust guided reverse process can achieve 17.22% increase in robust accuracy, which is significant.

**Comparison between PGD+EOT and AutoAttack:** Figure 3a and 3b show the comparison between PGD+EOT and AutoAttack on  $l_\infty$  and  $l_2$  threat models. Under different attacks, AT methods (Gowal et al., 2020, 2021; Pang et al., 2022) and AP methods (Yoon et al., 2021; Nie et al., 2022; Lee and Kim, 2023) exhibit significant differences in robust accuracy. AT performs better under PGD+EOT, while AP shows superior performance under AutoAttack. Typically, robustness evaluation is based on the worst-case results of the robust accuracy. Under this criterion, our method still outperforms all AT and AP methods. Furthermore, as compared to the second-best method on both attacks, our method improves the average robust accuracy by 6.39% against  $l_\infty$  and 1.16% against  $l_2$ , respectively.

**Accuracy-robustness trade-off:** Figure 3c shows the performance against AutoAttack  $l_2$  ( $\epsilon = 0.5$ ) threat models on CIFAR-10 with different weighting scales  $\lambda$ . We observe that as the weighting scale  $\lambda$  increasing, the robust accuracy increases while the standard accuracy decreases, which verifies our Equation (6) on the trade-off between robustness and accuracy.

## 6 Conclusion

In this paper, we propose an adversarial guided diffusion model (AGDM) for adversarial purification, which can enhance the robustness of diffusion models by a robust reverse process. Our innovative adversarial loss mechanism efficiently bypasses heavy computation of the entire reverse process in DMs during training and provides a practical solution to mitigate the accuracy-robustness trade-off. We conduct extensive experiments to empirically demonstrate that AGDM can significantly improve the robustness and generalization ability of diffusion-based purification.

**Limitations:** One of the limitations is that similar to previous works (Nie et al., 2022; Wang et al., 2022; Lee and Kim, 2023; Zhang et al., 2024), our proposed AGDM is also a time-consuming reverse process. In the experiments, evaluating the diffusion-based purifier against a single type of attack on 512 images requires  $\sim 13.8$  hours on 4-A5000 node. We leave the study of utilizing our robust guidance in more efficient and fast sampling strategies for future research.

## References

- Brian DO Anderson. Reverse-time diffusion equation models. *Stochastic Processes and their Applications*, 12(3):313–326, 1982.
- Anish Athalye, Logan Engstrom, Andrew Ilyas, and Kevin Kwok. Synthesizing robust adversarial examples. In *International conference on machine learning*, pages 284–293. PMLR, 2018.
- Maximilian Augustin, Alexander Meinke, and Matthias Hein. Adversarial robustness on in-and out-distribution improves explainability. In *European Conference on Computer Vision*, pages 228–245. Springer, 2020.
- Yatong Bai, Brendon G Anderson, Aerin Kim, and Somayeh Sojoudi. Improving the accuracy-robustness trade-off of classifiers via adaptive smoothing. *arXiv preprint arXiv:2301.12554*, 2023.
- Nicholas Carlini, Florian Tramer, Krishnamurthy Dj Dvijotham, Leslie Rice, Mingjie Sun, and J Zico Kolter. (certified!!) adversarial robustness for free! In *The Eleventh International Conference on Learning Representations*, 2023.
- Yair Carmon, Aditi Raghunathan, Ludwig Schmidt, John C Duchi, and Percy S Liang. Unlabeled data improves adversarial robustness. *Advances in neural information processing systems*, 32, 2019.
- Huanran Chen, Yinpeng Dong, Zhengyi Wang, Xiao Yang, Chengqi Duan, Hang Su, and Jun Zhu. Robust classification via a single diffusion model. *Proceedings of the 41st International Conference on Machine Learning*, 2024.
- Francesco Croce and Matthias Hein. Reliable evaluation of adversarial robustness with an ensemble of diverse parameter-free attacks. In *International conference on machine learning*, pages 2206–2216. PMLR, 2020.
- Francesco Croce, Maksym Andriushchenko, Vikash Sehwal, Edoardo DeBenedetti, Nicolas Flammarion, Mung Chiang, Prateek Mittal, and Matthias Hein. Robustbench: a standardized adversarial robustness benchmark. In *Thirty-fifth Conference on Neural Information Processing Systems Datasets and Benchmarks Track (Round 2)*, 2021.
- Francesco Croce, Sven Gowal, Thomas Brunner, Evan Shelhamer, Matthias Hein, and Taylan Cemgil. Evaluating the adversarial robustness of adaptive test-time defenses. In *International Conference on Machine Learning*, pages 4421–4435. PMLR, 2022.
- Jiequan Cui, Zhuotao Tian, Zhisheng Zhong, Xiaojuan Qi, Bei Yu, and Hanwang Zhang. Decoupled kullback-leibler divergence loss. *arXiv preprint arXiv:2305.13948*, 2023.
- Edoardo DeBenedetti, Vikash Sehwal, and Prateek Mittal. A light recipe to train robust vision transformers. In *2023 IEEE Conference on Secure and Trustworthy Machine Learning (SaTML)*, pages 225–253. IEEE, 2023.
- Jia Deng, Wei Dong, Richard Socher, Li-Jia Li, Kai Li, and Li Fei-Fei. Imagenet: A large-scale hierarchical image database. In *2009 IEEE conference on computer vision and pattern recognition*, pages 248–255. Ieee, 2009.
- Prafulla Dhariwal and Alexander Nichol. Diffusion models beat gans on image synthesis. *Advances in neural information processing systems*, 34:8780–8794, 2021.
- Gavin Weiguang Ding, Yash Sharma, Kry Yik Chau Lui, and Ruitong Huang. Mma training: Direct input space margin maximization through adversarial training. In *International Conference on Learning Representations*, 2019.
- Hadi M Dolatabadi, Sarah Erfani, and Christopher Leckie. l-inf robustness and beyond: Unleashing efficient adversarial training. In *European Conference on Computer Vision*, pages 467–483. Springer, 2022.
- Logan Engstrom, Andrew Ilyas, Hadi Salman, Shibani Santurkar, and Dimitris Tsipras. Robustness (python library), 2019. URL <https://github.com/MadryLab/robustness>.

- Ian J Goodfellow, Jonathon Shlens, and Christian Szegedy. Explaining and harnessing adversarial examples. *International Conference on Learning Representations*, 2015.
- Sven Gowal, Chongli Qin, Jonathan Uesato, Timothy Mann, and Pushmeet Kohli. Uncovering the limits of adversarial training against norm-bounded adversarial examples. *arXiv preprint arXiv:2010.03593*, 2020.
- Sven Gowal, Sylvestre-Alvise Rebuffi, Olivia Wiles, Florian Stimberg, Dan Andrei Calian, and Timothy A Mann. Improving robustness using generated data. *Advances in Neural Information Processing Systems*, 34:4218–4233, 2021.
- Kaiming He, Xiangyu Zhang, Shaoqing Ren, and Jian Sun. Deep residual learning for image recognition. In *Proceedings of the IEEE conference on computer vision and pattern recognition*, pages 770–778, 2016.
- Dan Hendrycks, Kimin Lee, and Mantas Mazeika. Using pre-training can improve model robustness and uncertainty. In *International conference on machine learning*, pages 2712–2721. PMLR, 2019.
- Jonathan Ho, Ajay Jain, and Pieter Abbeel. Denoising diffusion probabilistic models. *Advances in neural information processing systems*, 33:6840–6851, 2020.
- Xiaojun Jia, Yong Zhang, Baoyuan Wu, Ke Ma, Jue Wang, and Xiaochun Cao. Las-at: adversarial training with learnable attack strategy. In *Proceedings of the IEEE/CVF Conference on Computer Vision and Pattern Recognition*, pages 13398–13408, 2022.
- Mintong Kang, Dawn Song, and Bo Li. Diffattack: Evasion attacks against diffusion-based adversarial purification. In *Thirty-seventh Conference on Neural Information Processing Systems*, 2023.
- Dongjun Kim, Yeongmin Kim, Se Jung Kwon, Wanmo Kang, and Il-Chul Moon. Refining generative process with discriminator guidance in score-based diffusion models. *International Conference on Machine Learning*, 2023.
- Diederik Kingma, Tim Salimans, Ben Poole, and Jonathan Ho. Variational diffusion models. *Advances in neural information processing systems*, 34:21696–21707, 2021.
- Durk P Kingma and Prafulla Dhariwal. Glow: Generative flow with invertible 1x1 convolutions. *Advances in neural information processing systems*, 31, 2018.
- Alex Krizhevsky, Geoffrey Hinton, et al. Learning multiple layers of features from tiny images. *Technical Report*, 2009.
- Alexey Kurakin, Ian J Goodfellow, and Samy Bengio. Adversarial machine learning at scale. In *International Conference on Learning Representations*, 2016.
- C Laidlaw, S Singla, and S Feizi. Perceptual adversarial robustness: Defense against unseen threat models. In *International Conference on Learning Representations (ICLR)*, 2021.
- Minjong Lee and Dongwoo Kim. Robust evaluation of diffusion-based adversarial purification. In *Proceedings of the IEEE/CVF International Conference on Computer Vision (ICCV)*, pages 134–144, October 2023.
- Guang Lin, Chao Li, Jianhai Zhang, Toshihisa Tanaka, and Qibin Zhao. Adversarial training on purification (atop): Advancing both robustness and generalization. *arXiv preprint arXiv:2401.16352*, 2024.
- Aleksander Madry, Aleksandar Makelov, Ludwig Schmidt, Dimitris Tsipras, and Adrian Vladu. Towards deep learning models resistant to adversarial attacks. *International Conference on Learning Representations*, 2018a.
- Aleksander Madry, Aleksandar Makelov, Ludwig Schmidt, Dimitris Tsipras, and Adrian Vladu. Towards deep learning models resistant to adversarial attacks. In *International Conference on Learning Representations*, 2018b.

- Alexander Quinn Nichol, Prafulla Dhariwal, Aditya Ramesh, Pranav Shyam, Pamela Mishkin, Bob Mcgrew, Ilya Sutskever, and Mark Chen. Glide: Towards photorealistic image generation and editing with text-guided diffusion models. In *International Conference on Machine Learning*, pages 16784–16804. PMLR, 2022.
- Weili Nie, Brandon Guo, Yujia Huang, Chaowei Xiao, Arash Vahdat, and Anima Anandkumar. Diffusion models for adversarial purification. *International Conference on Machine Learning*, 2022.
- Tianyu Pang, Min Lin, Xiao Yang, Jun Zhu, and Shuicheng Yan. Robustness and accuracy could be reconcilable by (proper) definition. In *International Conference on Machine Learning*, pages 17258–17277. PMLR, 2022.
- Adam Paszke, Sam Gross, Francisco Massa, Adam Lerer, James Bradbury, Gregory Chanan, Trevor Killeen, Zeming Lin, Natalia Gimelshein, Luca Antiga, et al. Pytorch: An imperative style, high-performance deep learning library. *Advances in neural information processing systems*, 32, 2019.
- ShengYun Peng, Weilin Xu, Cory Cornelius, Matthew Hull, Kevin Li, Rahul Duggal, Mansi Phute, Jason Martin, and Duen Horng Chau. Robust principles: Architectural design principles for adversarially robust cnns. *British Machine Vision Conference (BMVC)*, 2023.
- Omid Poursaeed, Tianxing Jiang, Harry Yang, Serge Belongie, and Ser-Nam Lim. Robustness and generalization via generative adversarial training. In *Proceedings of the IEEE/CVF International Conference on Computer Vision*, pages 15711–15720, 2021.
- Sylvestre-Alvise Rebuffi, Sven Gowal, Dan A Calian, Florian Stimberg, Olivia Wiles, and Timothy Mann. Fixing data augmentation to improve adversarial robustness. *arXiv preprint arXiv:2103.01946*, 2021.
- Hadi Salman, Andrew Ilyas, Logan Engstrom, Ashish Kapoor, and Aleksander Madry. Do adversarially robust imagenet models transfer better? *Advances in Neural Information Processing Systems*, 33:3533–3545, 2020.
- Pouya Samangouei, Maya Kabkab, and Rama Chellappa. Defense-gan: Protecting classifiers against adversarial attacks using generative models. *International Conference on Learning Representations*, 2018.
- Lukas Schott, Jonas Rauber, Matthias Bethge, and Wieland Brendel. Towards the first adversarially robust neural network model on mnist. *International Conference on Learning Representations*, 2019.
- Vikash Sehwal, Saeed Mahloujifar, Tinashe Handina, Sihui Dai, Chong Xiang, Mung Chiang, and Prateek Mittal. Robust learning meets generative models: Can proxy distributions improve adversarial robustness? In *International Conference on Learning Representations*, 2021.
- Changhao Shi, Chester Holtz, and Gal Mishne. Online adversarial purification based on self-supervision. *International Conference on Learning Representations*, 2021.
- Yang Song and Stefano Ermon. Generative modeling by estimating gradients of the data distribution. *Advances in neural information processing systems*, 32, 2019.
- Yang Song, Taesup Kim, Sebastian Nowozin, Stefano Ermon, and Nate Kushman. Pixeldefend: Leveraging generative models to understand and defend against adversarial examples. *International Conference on Learning Representations*, 2018.
- Yang Song, Jascha Sohl-Dickstein, Diederik P Kingma, Abhishek Kumar, Stefano Ermon, and Ben Poole. Score-based generative modeling through stochastic differential equations. In *International Conference on Learning Representations*, 2020.
- Vignesh Srinivasan, Csaba Rohrer, Arturo Marban, Klaus-Robert Müller, Wojciech Samek, and Shinichi Nakajima. Robustifying models against adversarial attacks by langevin dynamics. *Neural Networks*, 137:1–17, 2021.

- David Stutz, Matthias Hein, and Bernt Schiele. Confidence-calibrated adversarial training: Generalizing to unseen attacks. In *International Conference on Machine Learning*, pages 9155–9166. PMLR, 2020.
- Christian Szegedy, Wojciech Zaremba, Ilya Sutskever, Joan Bruna, Dumitru Erhan, Ian Goodfellow, and Rob Fergus. Intriguing properties of neural networks. *International Conference on Learning Representations*, 2014.
- Jihoon Tack, Sihyun Yu, Jongheon Jeong, Minseon Kim, Sung Ju Hwang, and Jinwoo Shin. Consistency regularization for adversarial robustness. In *Proceedings of the AAAI Conference on Artificial Intelligence*, pages 8414–8422, 2022.
- Giorgio Ughini, Stefano Samele, and Matteo Matteucci. Trust-no-pixel: A remarkably simple defense against adversarial attacks based on massive inpainting. In *2022 International Joint Conference on Neural Networks (IJCNN)*, pages 1–10. IEEE, 2022.
- Jinyi Wang, Zhaoyang Lyu, Dahua Lin, Bo Dai, and Hongfei Fu. Guided diffusion model for adversarial purification. *arXiv preprint arXiv:2205.14969*, 2022.
- Zekai Wang, Tianyu Pang, Chao Du, Min Lin, Weiwei Liu, and Shuicheng Yan. Better diffusion models further improve adversarial training. *International conference on machine learning*, 2023.
- Eric Wong, Leslie Rice, and J Zico Kolter. Fast is better than free: Revisiting adversarial training. In *International Conference on Learning Representations*, 2019.
- Quanlin Wu, Hang Ye, and Yuntian Gu. Guided diffusion model for adversarial purification from random noise. *arXiv preprint arXiv:2206.10875*, 2022.
- QuanLin Wu, Hang Ye, Yuntian Gu, Huishuai Zhang, Liwei Wang, and Di He. Denoising masked autoencoders help robust classification. In *The Eleventh International Conference on Learning Representations*, 2023.
- Chaowei Xiao, Jun-Yan Zhu, Bo Li, Warren He, Mingyan Liu, and Dawn Song. Spatially transformed adversarial examples. In *International Conference on Learning Representations*, 2018.
- Chaowei Xiao, Zhongzhu Chen, Kun Jin, Jiongxiao Wang, Weili Nie, Mingyan Liu, Anima Anandkumar, Bo Li, and Dawn Song. Densepure: Understanding diffusion models for adversarial robustness. In *The Eleventh International Conference on Learning Representations*, 2023.
- Yuzhe Yang, Guo Zhang, Dina Katabi, and Zhi Xu. Me-net: Towards effective adversarial robustness with matrix estimation. *International Conference on Machine Learning*, 2019.
- Jongmin Yoon, Sung Ju Hwang, and Juho Lee. Adversarial purification with score-based generative models. In *International Conference on Machine Learning*, pages 12062–12072. PMLR, 2021.
- Sergey Zagoruyko and Nikos Komodakis. Wide residual networks. In *Proceedings of the British Machine Vision Conference 2016*. British Machine Vision Association, 2016.
- Hongyang Zhang, Yaodong Yu, Jiantao Jiao, Eric Xing, Laurent El Ghaoui, and Michael Jordan. Theoretically principled trade-off between robustness and accuracy. In *International conference on machine learning*, pages 7472–7482. PMLR, 2019.
- Jingfeng Zhang, Jianing Zhu, Gang Niu, Bo Han, Masashi Sugiyama, and Mohan Kankanhalli. Geometry-aware instance-reweighted adversarial training. In *International Conference on Learning Representations*, 2020.
- Mingkun Zhang, Jianing Li, Wei Chen, Jiafeng Guo, and Xueqi Cheng. Classifier guidance enhances diffusion-based adversarial purification by preserving predictive information, 2024. URL <https://openreview.net/forum?id=qvLPtx52ZR>.

## A Proofs of Adversarial Guided Diffusion Model (AGDM)

### A.1 Robust Reverse Process for DDPM

In the reverse process with adversarial guidance, similar to Dhariwal and Nichol (2021), we start by defining a conditional Markovian noising process  $\hat{q}$  similar to  $q$ , and assume that  $\hat{q}(y, x'|x_0)$  is an available label distribution and adversarial example (AE) for each image.

$$\begin{aligned}
\hat{q}(x_0) &:= q(x_0) \\
\hat{q}(y, x'|x_0) &:= \text{Label and AE per image} \\
\hat{q}(x_{t+1}|x_t, y, x') &:= q(x_{t+1}|x_t) \\
\hat{q}(x_{1:T}|x_0, y, x') &:= \prod_{t=1}^T \hat{q}(x_t|x_{t-1}, y, x').
\end{aligned} \tag{8}$$

When  $\hat{q}$  is not conditioned on  $\{y, x'\}$ ,  $\hat{q}$  behaves exactly like  $q$ ,

$$\begin{aligned}
\hat{q}(x_{t+1}|x_t) &= \int_{y, x'} \hat{q}(x_{t+1}, y, x'|x_t) dy dx' \\
&= \int_{y, x'} \hat{q}(x_{t+1}|x_t, y, x') \hat{q}(y, x'|x_t) dy dx' \\
&= \int_{y, x'} q(x_{t+1}|x_t) \hat{q}(y, x'|x_t) dy dx' \\
&= q(x_{t+1}|x_t) \int_{y, x'} \hat{q}(y, x'|x_t) dy dx' \\
&= q(x_{t+1}|x_t) \\
&= \hat{q}(x_{t+1}|x_t, y, x').
\end{aligned} \tag{9}$$

Following similar logic, we have:  $\hat{q}(x_{1:T}|x_0) = q(x_{1:T}|x_0)$  and  $\hat{q}(x_t) = q(x_t)$ . From the above derivation, it is evident that the conditioned forward process is identical to unconditioned forward process. According to Bayes rule, the reverse process  $\hat{q}$  satisfies  $\hat{q}(x_t|x_{t+1}) = q(x_t|x_{t+1})$ .

$$\begin{aligned}
\hat{q}(y, x'|x_t, x_{t+1}) &= \frac{\hat{q}(x_{t+1}|x_t, y, x') \hat{q}(y, x'|x_t)}{\hat{q}(x_{t+1}|x_t)} \\
&= \hat{q}(y, x'|x_t).
\end{aligned} \tag{10}$$

For conditional reverse process  $\hat{q}(x_t|x_{t+1}, y, x')$ ,

$$\begin{aligned}
\hat{q}(x_t|x_{t+1}, y, x') &= \frac{\hat{q}(x_t, x_{t+1}, y, x')}{\hat{q}(x_{t+1}, y, x')} \\
&= \frac{\hat{q}(x_t, x_{t+1}, y, x')}{\hat{q}(y, x'|x_{t+1}) \hat{q}(x_{t+1})} \\
&= \frac{\hat{q}(x_t|x_{t+1}) \hat{q}(y, x'|x_t, x_{t+1}) \hat{q}(x_{t+1})}{\hat{q}(y, x'|x_{t+1}) \hat{q}(x_{t+1})} \\
&= \frac{\hat{q}(x_t|x_{t+1}) \hat{q}(y, x'|x_t, x_{t+1})}{\hat{q}(y, x'|x_{t+1})} \\
&= \frac{\hat{q}(x_t|x_{t+1}) \hat{q}(y, x'|x_t)}{\hat{q}(y, x'|x_{t+1})} \\
&= \frac{q(x_t|x_{t+1}) \hat{q}(y, x'|x_t)}{\hat{q}(y, x'|x_{t+1})}.
\end{aligned} \tag{11}$$

Here  $\hat{q}(y, x'|x_{t+1})$  does not depend on  $x_t$ . Then, by assuming the label  $y$  and adversarial example  $x'$  are conditionally independent given  $x_t$ , we can rewrite the above equation as  $\hat{q}(x_t|x_{t+1}, y, x') = Z \cdot q(x_t|x_{t+1}) \hat{q}(x'|x_t) \hat{q}(y|x_t)$  where  $Z$  is a constant.

## A.2 Robust Reverse Process for Continuous-time Diffusion Models

In the main text, we only showcased the preliminaries and the corresponding robust reverse process related to DDPM, but our method can also be extended to continuous-time diffusion models (Song et al., 2020). The continuous-time DMs build on the idea of DDPM, employ stochastic differential equations (SDE) to describe the diffusion process as follows,

$$dx = f(x, t)dt + G(t)dw, \quad (12)$$

where  $w$  represents a standard Brownian motion,  $f(x, t)$  represents the drift of  $x_t$  and  $G(t)$  represents the diffusion coefficient.

By starting from sample of Eq. 12 and reversing the process, Song et al. (2020) run backward in time and given by the reverse-time SDE,

$$dx = [f(x, t) - G(t)^2 \nabla_x \log p_t(x)]dt + G(t)d\bar{w}, \quad (13)$$

where  $\bar{w}$  represents a standard reverse-time Brownian motion and  $dt$  represents the infinitesimal time step. Similar to DDPM, the continuous-time diffusion model also requires training a network to estimate the time-dependent function  $\nabla_x \log p_t(x)$ . One common approach is to use a score-based model  $s_\theta(x, t)$  (Song et al., 2020; Kingma et al., 2021). Subsequently, the reverse-time SDE can be solved by minimizing the score matching loss (Song and Ermon, 2019),

$$\mathcal{L}_\theta = \int_0^T \lambda(t) \mathbb{E}[\|s_\theta(x_t, t) - \nabla_{x_t} \log p_{0t}(x_t|x_0)\|^2] dt, \quad (14)$$

where  $\lambda(t)$  is a weighting function, and  $p_{0t}$  is the transition probability from  $x_0$  to  $x_t$ , where  $x_0 \sim p_0(x)$  and  $x_t \sim p_{0t}(x_t|x_0)$ .

In the robust reverse process of continuous-time DMs, similar to Song et al. (2020), we suppose the initial state distribution is  $p_0(x(0) | y, x')$  based on Eq. 13. Subsequently, using Anderson (1982) for the reverse process, we have

$$dx = \{f(x, t) - \nabla \cdot [G(t)G(t)^T] - G(t)G(t)^T \nabla_x \log p_t(x|y, x')\} dt + G(t)d\bar{w}. \quad (15)$$

Given a diffusion process  $x_t$  with SDE and score-based model  $s_{\theta^*}(x, t)$ , we first observe that

$$\nabla_x \log p_t(x_t|y, x') = \nabla_x \log \int p_t(x_t|y_t, y, x') p(y_t|y, x') dy_t, \quad (16)$$

where  $y_t$  is defined via  $x_t$  and the forward process  $p(y_t | x_t)$ . Following the two assumptions by Song et al. (2020):  $p(y_t | y, x')$  is tractable;  $p_t(x_t|y_t, y, x') \approx p_t(x_t|y_t)$ , we have

$$\begin{aligned} \nabla_x \log p_t(x_t|y, x') &\approx \nabla_x \log \int p_t(x_t|y_t) p(y_t|y, x') dy_t \\ &\approx \nabla_x \log p_t(x_t|\hat{y}_t) \\ &= \nabla_x \log p_t(x_t) + \nabla_x \log p_t(\hat{y}_t|x_t) \\ &\approx s_{\theta^*}(x_t, t) + \nabla_x \log p_t(\hat{y}_t|x_t), \end{aligned} \quad (17)$$

where  $\hat{y}_t$  is a sample from  $p(y_t|y, x')$ . Then, by assuming the label  $y$  and adversarial example  $x'$  are conditionally independent given  $x_t$ , we can update Eq. 13 with above formula, and obtain a new denoising model  $\bar{\epsilon}$  with the guidance of label  $y$  and adversarial example  $x'$ ,

$$dx_t = [f(x, t) - G^2(t)(\nabla_x \log p_t(x) + \nabla_x \log p_t(y|x) + \nabla_x \log p_t(x'|x))(x, t)] dt + G(t) d\bar{w}. \quad (18)$$

### A.3 The Algorithm of Robust Reverse Process

---

**Algorithm 1** Adversarial guided diffusion model, given a diffusion model  $(\mu_\theta(x_t, t), \sigma_t)$  and scale  $s$ .

---

**Input:** Adversarial examples  $x'$   
**Output:** Purified examples  $x_0$   
 $x_{t^*} \leftarrow$  sample from Equation (7)  
**for**  $t$  from  $t^*$  to 1 **do**  
     $\mu, \Sigma \leftarrow \mu_\theta(x_t, t), \sigma_t$   
     $x_{t-1} \leftarrow$  sample from  $\mathcal{N}(\mu + s\Sigma\nabla_{x_t} \log p_\phi(y | x_t) - s\Sigma\nabla_{x_t} \mathcal{D}(f_\phi(x'), f_\phi(x_t)), \Sigma)$   
**end for**  
**return**  $x_0$

---

## B Comparison with AGDM and AToP

To Enhance the existing pre-trained generator-based purification architecture to further improve robust accuracy against attacks. Lin et al. (2024) propose adversarial training on purification (AToP). Based on pre-trained model, they redesign the loss function to fine-tune the purifier model using adversarial loss.

Pre-training stage:

$$L_{\theta_g} = L_g(x, \theta_g). \quad (19)$$

Fine-tuning stage:

$$L_{\theta_g} = L_g(x', \theta_g) + s \cdot L_{cls}(x', y, \theta_g, \theta_f) = L_g(x', \theta_g) + s \cdot \max_{\delta} CE \{y, f(g(x', \theta_g))\}, \quad (20)$$

where  $L_g$  represents the original generative loss function of the generator model, which trained on clean examples and generates images similar to clean examples. During fine-tuning, AToP input the adversarial examples  $x'$  to optimize generator with generative loss, and further optimize the generator model with the adversarial loss  $L_{cls}$ , which is the cross-entropy loss between the output of  $x'$  and the ground truth  $y$ . However, training the generator with adversarial examples can lead to a decline in the performance on clean examples, thereby reducing standard accuracy. To address this issue, we modify back the input as  $x$  in two terms of  $L_{\theta_g}$  and introduce a new constraint  $L_{dis}$  to enhance robust accuracy. To facilitate clearer comparison, we have used the same notation as AToP to represent our loss function, which differs from actual loss function.

$$\begin{aligned} L_{\theta_g} &= L_g(x, \theta_g) + s_1 \cdot L_{cls}(x, y, \theta_g, \theta_f) + s_2 \cdot L_{dis}(x, x', \theta_g, \theta_f) \\ &= L_g(x, \theta_g) + s_1 \cdot CE \{y, f(g(x, \theta_g))\} + s_2 \cdot KL \{f(g(x, \theta_g)), f(g(x', \theta_g))\}. \end{aligned} \quad (21)$$

Distinct from Eq. 20, in Eq. 21 we revert the input of the first two terms back to the clean examples  $x$ . By increasing the weight of  $s_1$ , we can improve the standard accuracy on clean examples. Additionally, we introduce a new constraint term  $L_{dis}$ , which is the KL divergence between the feature map from the clean example  $x$  and the adversarial example  $x'$ . By increasing the weight of  $s_2$ , we can improve the robust accuracy on adversarial examples. This effectively mitigates the accuracy-robustness trade-off issue.

## C Visualization



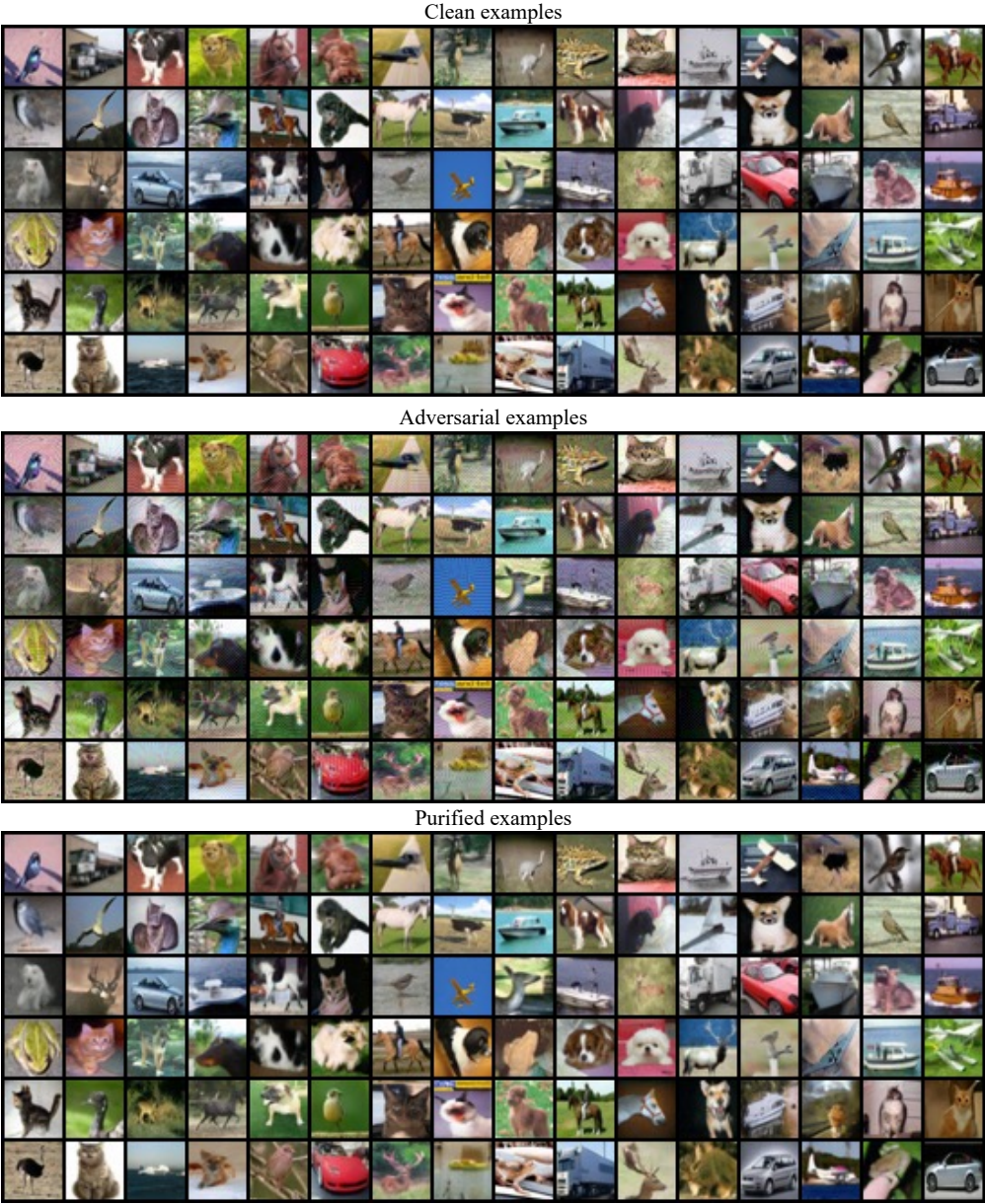
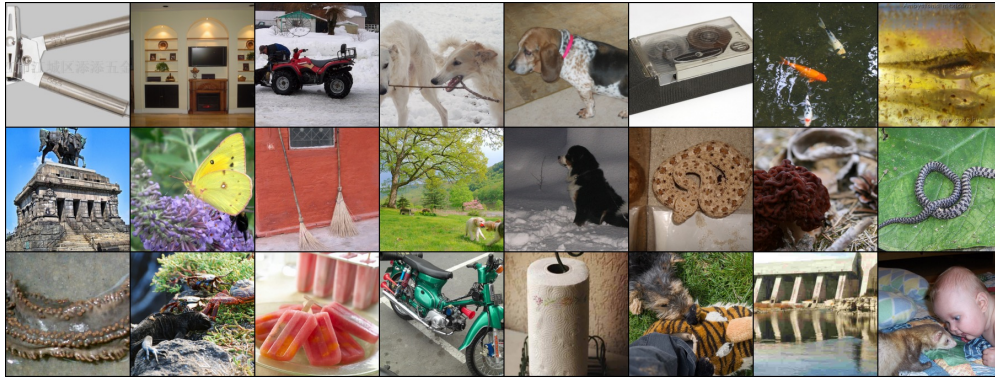
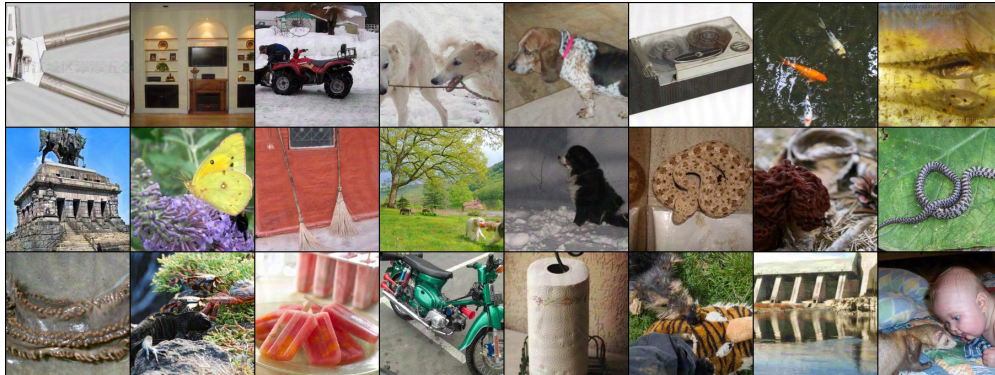


Figure 4: Clean examples (Top), adversarial examples (Middle) and purified examples (Bottom) of CIFAR-10.

Clean examples



Adversarial examples



Purified examples

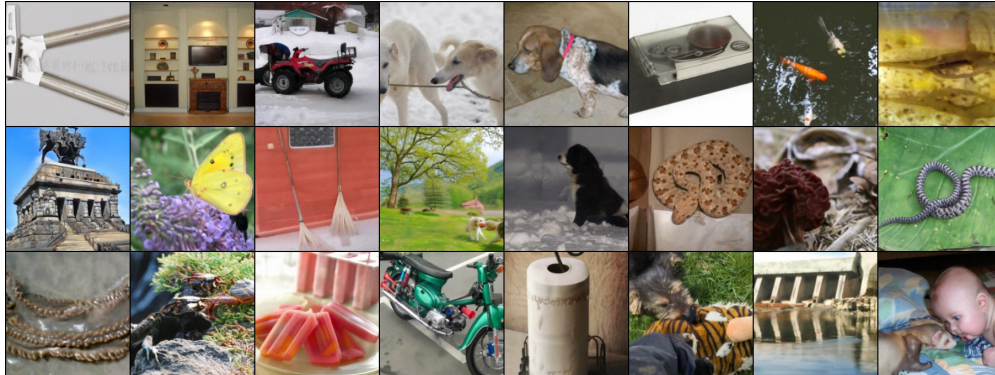


Figure 5: Clean examples (Top), adversarial examples (Middle) and purified examples (Bottom) of ImageNet.